

Strengthening effect of crushed rock revetment and thermosyphons in a traditional embankment in permafrost regions under warming climate

MEI Qi-Hang^{a,b}, CHEN Ji^{a,b,*}, WANG Jin-Chang^c, HOU Xin^{a,b}, ZHAO Jing-Yi^a,
ZHANG Shou-Hong^c, DANG Hai-Ming^c, GAO Jia-Wei^{a,b}

^a Beiluhe Observation and Research Station of Frozen Soil Engineering and Environment, State Key Laboratory of Frozen Soil Engineering, Northwest Institute of Eco-Environmental and Resources, Chinese Academy of Sciences, Lanzhou, 730000, China

^b University of Chinese Academy of Sciences, Beijing, 100049, China

^c China Railway Qinghai-Tibet Group Co. Ltd, Xining, 810007, China

Received 22 June 2020; revised 31 August 2020; accepted 12 January 2021

Available online 2 February 2021

Abstract

The embankment of the Qinghai–Tibet Railway (QTR) has been experiencing severe problems due to permafrost degradation, especially in warm and ice-rich permafrost regions. Based on ground temperature and deformation data of the embankment at location K1497 + 150 of the QTR in 2006–2018, the thermal regime and deformation process were analysed. The results showed that 1) the degradation rate of permafrost under the embankment was faster than that under the natural site without engineering construction, and 2) the deformation rate of the embankment had exceeded the safety range for the QTR embankment before adopting mitigative measures. In addition, this study evaluated the cooling effect on the underlying permafrost and working mechanism of two strengthening measures. Two measures, crushed rock revetment (CRR) and thermosyphons, were adopted to protect the underlying permafrost from continual degradation. The individual cooling effect of the CRR was not as good as that of the thermosyphons. However, the combination of the two could enhance the protective effects of each on the underlying permafrost, effectively cooling the permafrost and improving the stability of the embankment.

Keywords: Climate warming; Permafrost; Crushed rock revetment (CRR); Thermosyphons; Settlement

1. Introduction

The Qinghai–Tibet Railway (QTR) crosses 550 km of continuous permafrost regions on the Qinghai–Tibet Plateau (QTP), and 134 km of the QTR extends into warm and ice-rich permafrost areas. Here, warm means that permafrost has a mean annual ground temperature (MAGT) varying between

–1 and 0 °C, and ice-rich means the ice content of permafrost is more than 20% by volume. Since its operation on July 1, 2006, the QTR has played an important role in the development of the economy and tourism (Wu et al., 2002; Li et al., 2016, 2018). However, field monitoring results show that the permafrost along the QTR has been degrading because of natural and human activities, such as climate warming and roadbed construction. The degradation of permafrost is worse in warm and ice-rich permafrost regions, which in turn, is threatening the safe operation of the QTR (Cheng, 2002; Wu et al., 2011; Wu and Niu, 2013; Peng et al., 2015; Yu et al., 2016; Zhang et al., 2020).

Considering the QTR designed for 100-years of operation and combining the construction experience from the existing Qinghai–Tibet highway and other infrastructures on the QTP,

* Corresponding author. Beiluhe Observation and Research Station of Frozen Soil Engineering and Environment, State Key Laboratory of Frozen Soil Engineering, Northwest Institute of Eco-Environmental and Resources, Chinese Academy of Sciences, Lanzhou, 730000, China.

E-mail address: chenji@lzb.ac.cn (CHEN J.).

Peer review under responsibility of National Climate Center (China Meteorological Administration).

the proactive cooling measures, such as crushed rocks, ventilation ducts, and thermosyphons, were adopted at different parts of the QTR according to the permafrost type (Cheng and He, 2001; Cheng, 2005; Ma et al., 2009). The cooling mechanism of crushed rock revetment (CRR) involves a crushed rock layer insulating against exterior heat, preventing it from entering the embankment during the warm season and accelerating heat loss from the ground to the environment through air convection during the cold season (Mu et al., 2018; Zhao et al., 2019). Accordingly, the CRR could reduce the heat accumulation in the embankment over time. Thermosyphon is an environmental protection measure that can quickly lower the embankment temperature by taking advantage of the temperature difference between the evaporator and condenser sections without requiring extra energy (Wen et al., 2005; Yan et al., 2019). However, some parts of the QTR have no cooling measures because of the high cost. Permafrost degradation and the resulting embankment deformation, at the parts without any cooling measures have increased significantly, especially in areas of warm and ice-rich permafrost (Wu et al., 2007; Mu et al., 2012; Sun et al., 2018).

Studies on the permafrost changes along the QTP have indicated that the boundary between island permafrost and continuous permafrost on the QTP has moved northward by approximately 12 km because of climate warming, and the permafrost extent will continue to decrease in the future (Wang et al., 2000; Cheng and Wu, 2007; Wu and Zhang, 2008; Ran et al., 2018). Thus, it is necessary to adopt cost-effective measures to regain control of the deformation of the embankment and maintain its stability in permafrost regions. Field monitoring of the ground temperature and measurements of the deformation of the embankment in section DK1139 + 780 of the QTR show that the combined application of the CRR and thermosyphons on the embankment can effectively improve its stability without considering the change of weather conditions (Ma et al., 2012). Another analysis, based on field monitoring of ground temperatures, has indicated that the application of the CRR in duct-ventilated embankments is beneficial in cooling the underlying permafrost and reducing the temperature difference between the sunny and shady shoulders of the embankment (Hou et al., 2015a). By establishing a coupled strengthening model for three cases, it has been shown that the combination of the CRR and thermosyphons is the most effective strengthening measure, especially when the thermosyphons are set at an angle (Hou et al., 2018). By comparing the thermal regime changes of thermally insulated embankment and traditional embankment, previous researchers have also found that the protective effect of the CRR on the embankment and the underlying permafrost is not as good as the thermosyphons in a warm permafrost region (Hou et al., 2015b). Considering future engineering requirements, it is necessary to further study the cooling effect of the CRR and thermosyphons on the embankment and explore their criteria for application.

In this study, the stability of the embankment with the CRR and thermosyphons in warm and ice-rich permafrost regions was analysed based on measurements of the thermal regime

and the deformation of the embankment; the cooling effects of these two measures are discussed by comparing the traditional embankment without these measures. Finally, the feasibility of applying the strengthening measures to the embankment is discussed. This study provides a reference for embankment design, such as jointly using CRR and thermosyphons, in warm permafrost regions in a warming climate.

2. Data and method

2.1. Site description

The study embankment section is situated at the mileage of K1497 + 150 along the QTR in the interior of the QTP. Topographically, this section is located in the Amdo valley, which is on the southern side of the Tanggula Mountains. This site is very close to the southern lower limit of continuous permafrost on the QTP (Fig. 1). The embankment is located on a slope with a gradient of 9% from south to north. A geological survey of this section conducted in November 2004 indicated a permafrost thickness of more than 13.7 m, of which 1.1 m was ice-saturated frozen soil with more than a 40% volumetric ice content, and the rest was ice-poor frozen soil with less than a 10% volumetric ice content. Field monitoring data showed that the permafrost table at the natural site near the embankment was 2.3 m and the MAGT was -0.09°C in 2006. A field investigation in the summer of 2018 showed vegetation coverage of approximately 80%–90%. Thermokarst depressions and ponds were distributed widely, and the largest one was over 10 m in diameter.

As shown in Fig. 2a, the left and right (according to the direction from Golmud to Lhasa) shoulders of the embankment are 3.1 m and 2.9 m high, respectively. The orientation of the embankment is approximately 185° in azimuth degrees, resulting in a slight slope orientation effect, which has caused a differential distribution of ground temperatures and deformation of the embankment. When the embankment was built in 2003, there were no proactive measures installed. As a result, a settlement of 0.6 m was observed in this section between 2006 and 2010. Then, the CRR in May 2010 and inclined thermosyphons in November 2012 were installed to prevent further settlement. The CRR is made up of a crushed-rock layer approximately 1 m thick, in which the dimensions of crushed rocks vary from 30 to 40 cm in diameter. The thermosyphons, 9 m-long in total, include a 6 m evaporation section. They are distributed at the slope toes on both sides of the embankment in a single row and are 3.25 m apart.

2.2. The monitoring system and the measurements

As part of the long-term monitoring program of the QTR, the ground temperatures and deformation of the embankment have been monitored in this section since November 2005. In total, there are three boreholes with temperature monitoring equipment, and their depths are 15, 20 and 20 m. The two boreholes with depths of 20 m are located in the side shoulders of the embankment and are used to monitor changes of ground

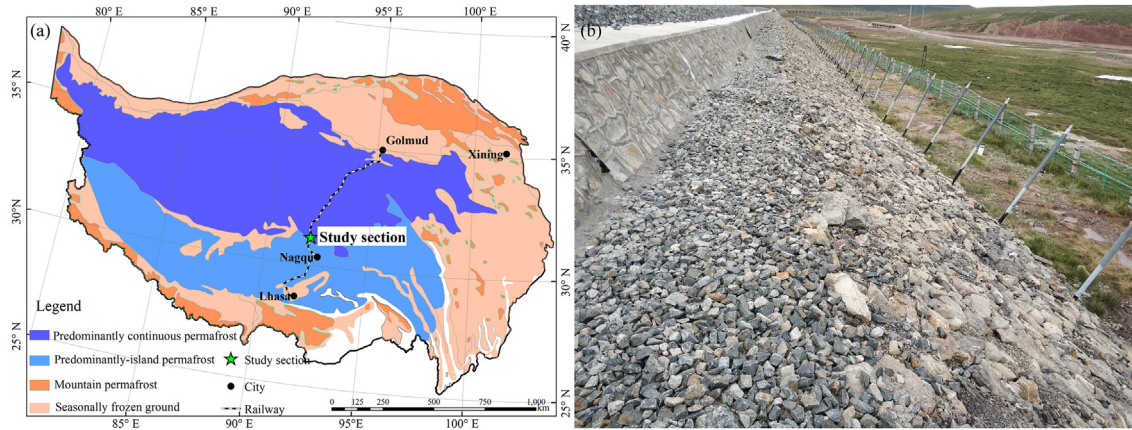


Fig. 1. Location (a) and photo (b) of section K1497 + 150 at Amdo along the Qinghai–Tibet Railway from Golmud, Qinghai to Lhasa, Tibet China (The base map of (a) is from Shi and Mi (2018)).

temperatures at different depths under the embankment. The borehole with a depth of 15 m is located approximately 20 m away from the left slope toe of the embankment and is used to monitor temperature changes at different depths under the natural site (Fig. 2a). The purpose of the 15 m deep borehole which is far from the embankment, is to reflect temperature changes that are only influenced by the climate. The temperature sensors have an accuracy of ± 0.05 °C and are distributed at 0.5 m intervals from the ground surface down to 10 m and at 1 m intervals after 10 m. Damage to the sensors from the weather and animals explains the missing ground temperature data at depths of 0–1 m in the natural borehole.

The monitoring system for the embankment deformation contains 10 sensing points: a datum point, 3 middle points and 6 side points (Fig. 2b). The datum point (P) is located at the top of a steel pipe that is static and buried 20 m under the shoulder. Three middle points (M1–M3) are fixed and marked on the railway sleepers. Six side points (L1–L3 and R1–L3) are steel nails fixed 20 cm under the embankment surface. The temperature is measured daily and recorded automatically in a data log, whereas the deformation is measured manually monthly using the optical level. To ensure the integrity of each freeze–thaw cycle during the study, data collected from January 2006 to December 2018 were used. The permafrost table was calculated using a linear interpolation of the ground temperatures between two neighbouring points above and below 0 °C (Wu and Zhang, 2010). To simplify the statistics, the MAGT refers to the ground temperature at 15 m below the surface.

3. Results

3.1. Permafrost change at the natural site

From 2006 to 2018, the ground temperatures on October 15th (when the annual maximum thaw occurs) at the natural site increased remarkably at all depths (Fig. 3). At a depth of 3 m, which is close to the permafrost table, the annual increment is 0.061 °C in 2018, which is only 0.009 °C in

2006, where the ground temperature increased by 0.31 °C. The increase of the permafrost temperature at other depths was between 0.09 °C and 0.18 °C, all of which were less than that at 3 m.

The active layer thickness (ALT), defined as the mean annual maximum thaw depth of the permafrost layer, at the natural site increased from 2.31 m in 2006 to 3.02 m in 2018 with an average rate of 0.055 m per year, indicating that the permafrost table decreased by 0.71 m during the observed 13 years (Fig. 4). The MAGT increased from -0.086 °C to 0.083 °C, and the warming rate increased significantly with time. In 2015, the MAGT at the natural site was above 0 °C, indicating that the permafrost base had already risen to above 15 m. Finally, the permafrost base rose to 12.9 m in 2018.

3.2. Variations in the thermal regime of the embankment

In 2006, three years after construction of the roadbed, there was a thawed interlayer under the left shoulder, which created a large difference between the temperature fields of the left and right shoulders (Fig. 5). The existence of the thawed interlayer would lead to an accelerating descending of the permafrost table, and eventually cause deformation of the embankment (Wang et al., 2018). From 2006 to 2009, the permafrost table under the left shoulder decreased by 0.36 m at an average rate of 0.090 m per year, and the ALT was basically stable. After the installation of CRR, the decline rate of the permafrost table decreased to 0.012 m per year in 2010–2012. And after the addition of the thermosyphons, the permafrost table elevated at a rate of 0.038 m per year in 2013–2018.

Under the right shoulder, the changes of the permafrost temperature showed the same trend as for the left shoulder from 2006 to 2016 (Fig. 5b).

The ground temperature at a depth of 1.5 m at the natural site varied dramatically with seasons (Fig. 6a). The long-term change of the ground temperature shows a trend of a continual increase in annual amplitude, characterized by the highest temperature increase and the lowest decrease. Moreover, the

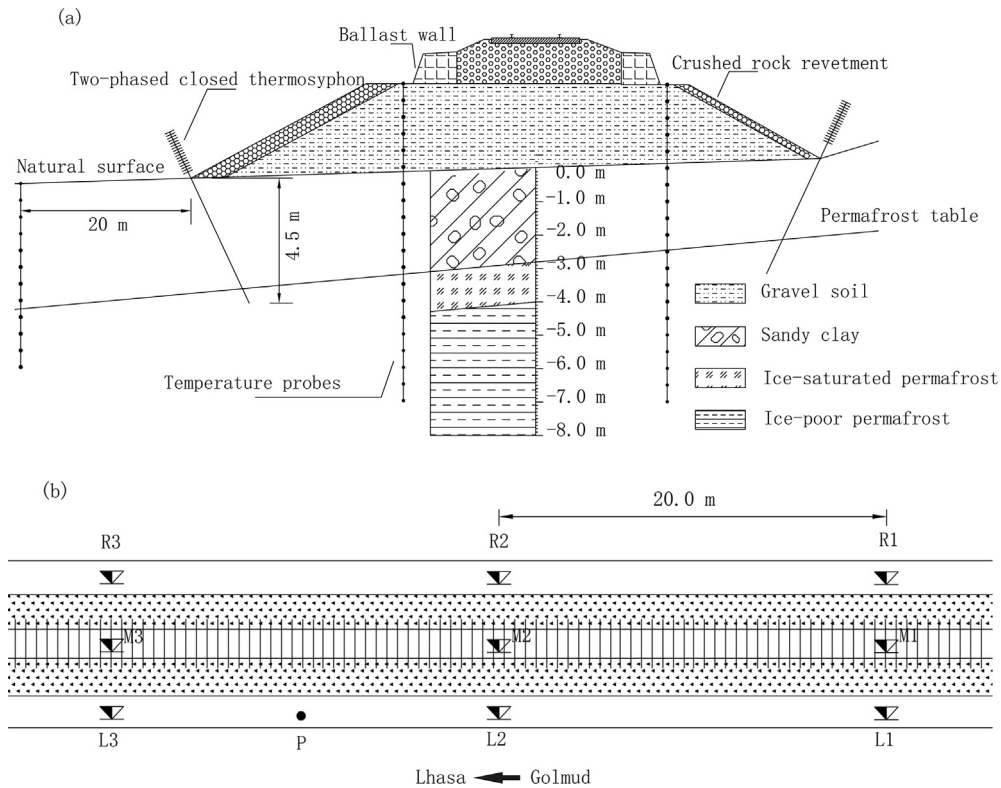


Fig. 2. Monitoring system for the ground temperatures (a), and the deformation of the embankment (b) at section K1497 + 150 along the Qinghai–Tibet Railway.

varying amplitude of the highest temperature is larger than that of the lowest temperature, which contributed to the continuous increase of the mean annual temperature of the permafrost. There was no significant change in the ground temperature from 2006 to 2010 under the left shoulder (Fig. 6b). After the CRR was installed, the annual amplitude of the ground temperature significantly decreased, with the highest temperature falling from 7.7 °C in 2009 to 4.5 °C in 2011, and the lowest temperature increasing from -4.5 °C in 2009 to -4.0 °C in 2011. The annual amplitude of the ground temperature at the right shoulder decreased after installation of the CRR, similar to the left shoulder (Fig. 6c).

At a depth of 6 m under the natural site, the ground temperature of the permafrost increased at a rate of 0.008 °C per year in 2006–2018 (Fig. 7). However, the thermal regime of the soil under the embankment strengthened by the CRR and the thermosyphons showed more complicated characteristics than the soil under the natural site. From 2006 to 2009, the soil under the left shoulder was warming, with the lowest and highest ground temperatures rising by 0.03 °C and 0.24 °C, respectively. After the CRR was installed in 2010, the lowest ground temperature at 6 m depth under the left shoulder appeared stable, and the highest ground temperature decreased rapidly by more than 0.41 °C. The ground temperature under the right shoulder stopped rising and stabilized at approximately -0.07 °C. However, the degradation rate of the permafrost at deep layers decreased slightly but did not completely stop after installation of the CRR (Fig. 8). From January 2006 to November 2012, the annual increase of

permafrost temperature below the left shoulder at depths of 8 m and 12 m decreased from 0.017 °C and 0.016 °C to 0.008 °C and 0.007 °C respectively. On the right shoulder of the embankment, the annual increase decreased from 0.018 °C and 0.01 °C in 2006 to 0.006 °C and 0.007 °C in 2012 at depths of 8 m and 12 m respectively.

After installation of the thermosyphons at the end of 2012, the mean annual temperature at 6 m depth under the left and right shoulders decreased by 0.02 °C and 0.13 °C respectively from 2012 to 2015 (Fig. 7). At a depth of 8 m, the changes of

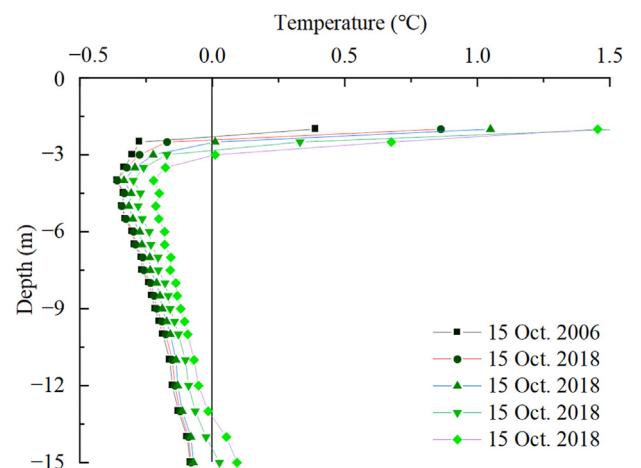


Fig. 3. Ground temperature profiles on Oct. 15th at the natural site in different years.

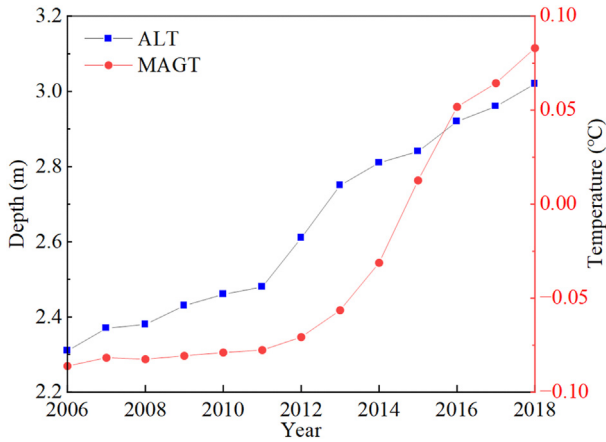


Fig. 4. Variations in the active layer thickness (ALT) and mean annual ground temperature (MAGT) at the natural site in 2006–2018.

the ground temperature caused by the thermosyphons was more serious (Fig. 8a). The ground temperatures under the left and right shoulders of the embankment both rose at 0.014 °C per year from 2006 to 2012, which was higher than the rising rate of 0.009 °C per year of the natural site at the same depth. After installation of the thermosyphons, the mean annual temperature decreased by 0.07 °C on the left and by 0.31 °C on the right from 2013 to 2018 at a depth of 8 m below the embankment. In 2018, five years after the installation of the thermosyphons, the lowest temperature on the right side was 0.4 °C lower than that on the left.

From 2006 to 2018, the natural site was warming at a rate of 0.009 °C per year at a depth of 12 m. The warming rates of the permafrost under the left and the right shoulders were 0.012 °C per year and 0.009 °C per year from 2006 to 2012 (Fig. 8b). After the thermosyphons were installed, the mean annual temperature under the left and right shoulders decreased by approximately 0.08 °C and 0.09 °C respectively from 2013 to 2018. In 2015, the temperature of permafrost under the left and right shoulders began to be lower than that of the natural site.

3.3. Deformation characteristics of the embankment

From 2006 to 2018, the cumulative deformation of all the monitoring points on both sides of the embankment was between 40.6 and 69.9 cm (Fig. 9). The deformation rate of this embankment was not constant at most of the monitoring points. For example, at points L3 and R3, which are symmetrically distributed along the centre line of the roadbed, the deformation rate gradually decreased. From January 2006 to April 2010, the cumulative deformations at points L3 and R3 were 31.5 cm and 36.4 cm, respectively, and the deformation rates were 7.27 cm per year and 8.4 cm per year. These numbers exceeded the maximum permissible standards of the designing code, which are 20 cm and 5 cm per year, respectively. After the CRR and thermosyphons were installed in 2010 and 2012, respectively, the deformation rate of the embankment noticeably decreased. The cumulative deformation at point L3 and R3 were 2.2 cm and 10.2 cm, from 2013

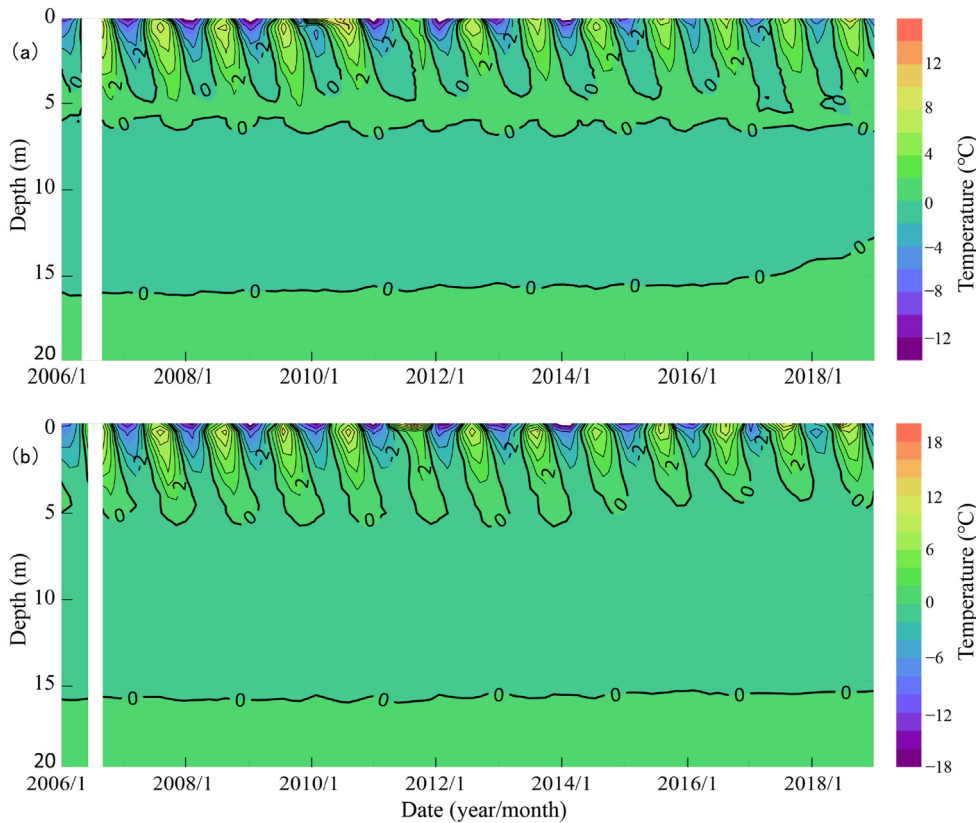


Fig. 5. Isotherms of the ground temperature at the left shoulder (a) and the right shoulder (b).

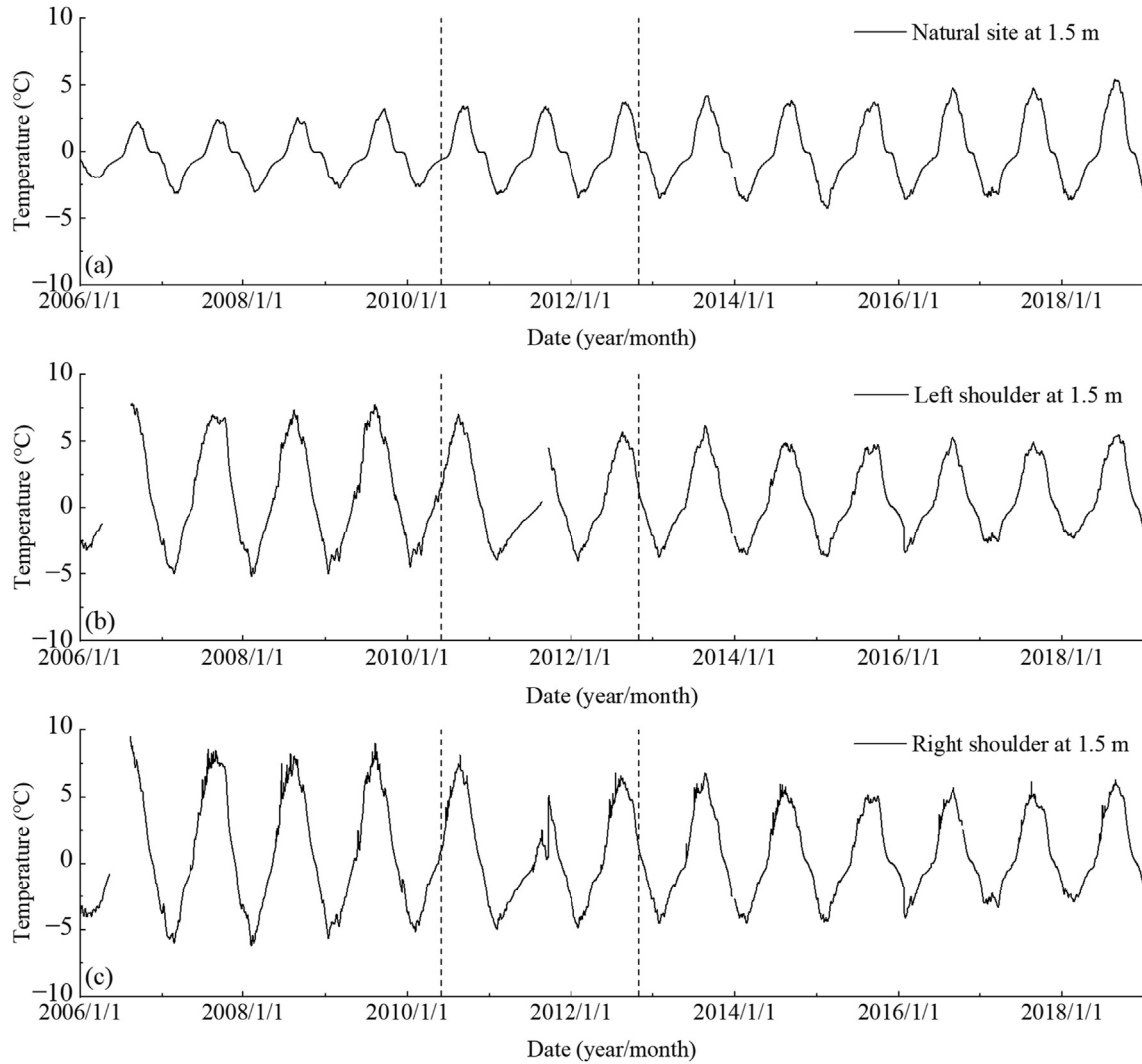


Fig. 6. Variations in the ground temperatures at different boreholes in 2006–2018 (In Fig. 6–8, the two dotted lines denote the addition of the CRR in 2010 and the thermosiphon in 2012 respectively).

to 2018 with corresponding deformation rates of 0.37 cm per year and 1.7 cm per year, respectively; these final deformation rates are within the requirements of the design code. However, the settlement rate at point L2 was 5.33 cm per year from 2016 to 2018, which was higher than that from 2010 to 2015. Therefore, deformation monitoring at this point should be performed more frequently to determine whether more measures should be taken.

At sections of the railway where serious settlement deformation happened or is happening, gravel was used to fill the space under the railway sleepers to maintain the level of the railway. Therefore, the deformation at the middle points on the sleeper consisted of two parts; one from the embankment settlement and another from the filled gravel layer (Fig. 10). The settlement deformation process at the middle points had the same characteristics as those at the side of the embankment. At the middle point, M3, gravel was refilled 9 times between 2006 and 2018, and the refilled gravel layer reached 40.4 cm thick. Before 2013, it was refilled 5 times, achieving a

thickness of 27.0 cm. After 2013, the gravel was refilled 4 times, adding 13.0 cm.

4. Discussion

Analysis on the ground temperatures at section K1497 + 150 along the QTR indicated that the cooling effects from the CRR and thermosiphons on the embankment both, to some degree, slowed the degradation of permafrost under the embankment. After application of the CRR in 2010, the highest ground temperature at a depth of 1.5 m under the left shoulder decreased by 3.3 °C, whereas the minimum ground temperature increased by 0.5 °C. The lowest ground temperature at a depth of 6 m did not change significantly in the cold season, whereas the maximum temperature decreased over 0.41 °C in the warm season. The difference in the ground temperature at depths of 1.5 m and 6 m under the left shoulder showed that, in section K1497 + 150, the CRR prevents the embankment from warming up mainly by the thermal

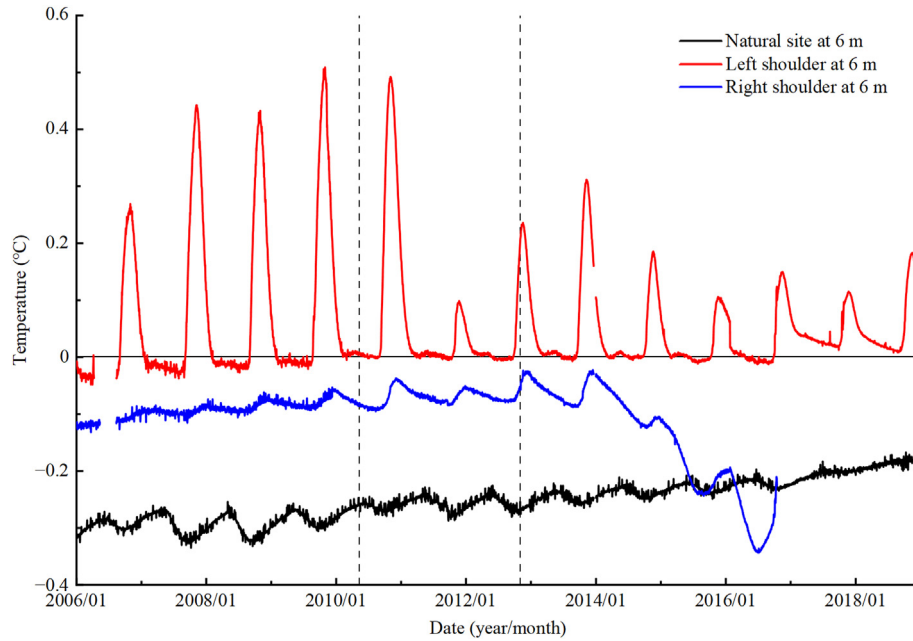


Fig. 7. Variations of the ground temperature in different boreholes in 2006–2018.

insulation effect in the warm season, which is different from the expectation that the forced convection effect in the cold season would play a more important role. Measurements of the ground temperatures at depths of 8 m and 12 m indicated that the degradation rate of the permafrost at deep layers decreased after the application of the CRR but did not cease completely, as shown in Fig. 8. The present study shows that application of only the CRR could not completely prevent permafrost degradation and improve the stability of the embankment in

ice-rich and warm permafrost regions. Long term monitoring data on embankments with crushed rock structures in different permafrost regions proved that the cooling effect from the crushed rock structure decreased with the increase of the MAGT (Ma et al., 2008). After installation the thermosyphons, the ground temperatures at depths of 8 m and 12 m changed from increasing to decreasing, proving that the thermosyphons were able to cool the permafrost mainly in the cold season (Fig. 8). The combination of the thermal insulation

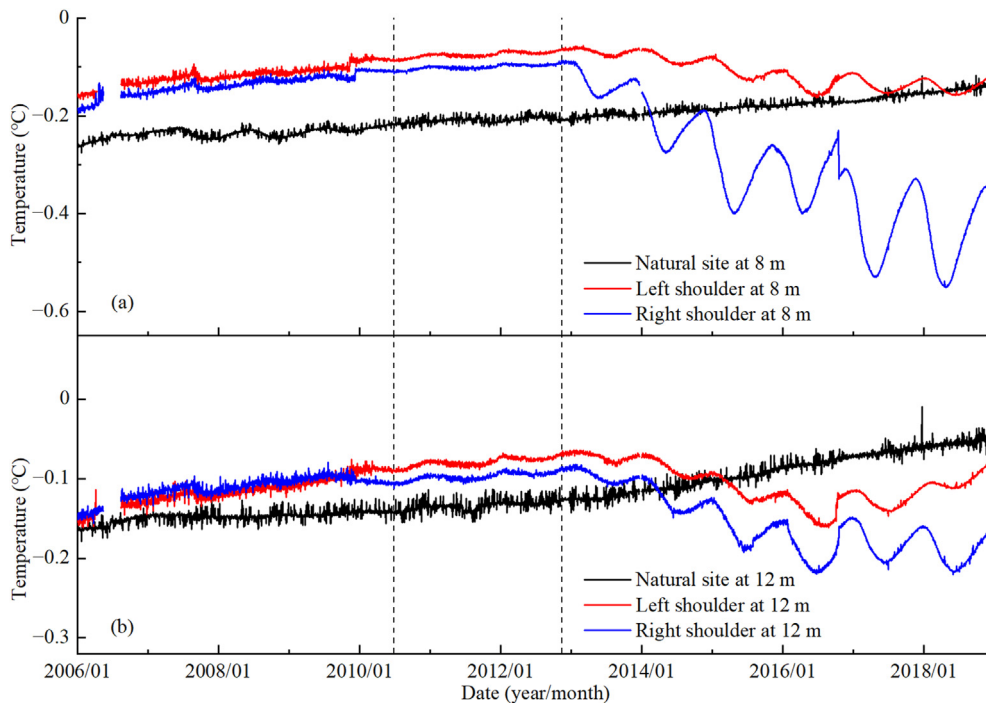


Fig. 8. Variations in the ground temperature at different boreholes in 2006–2018.

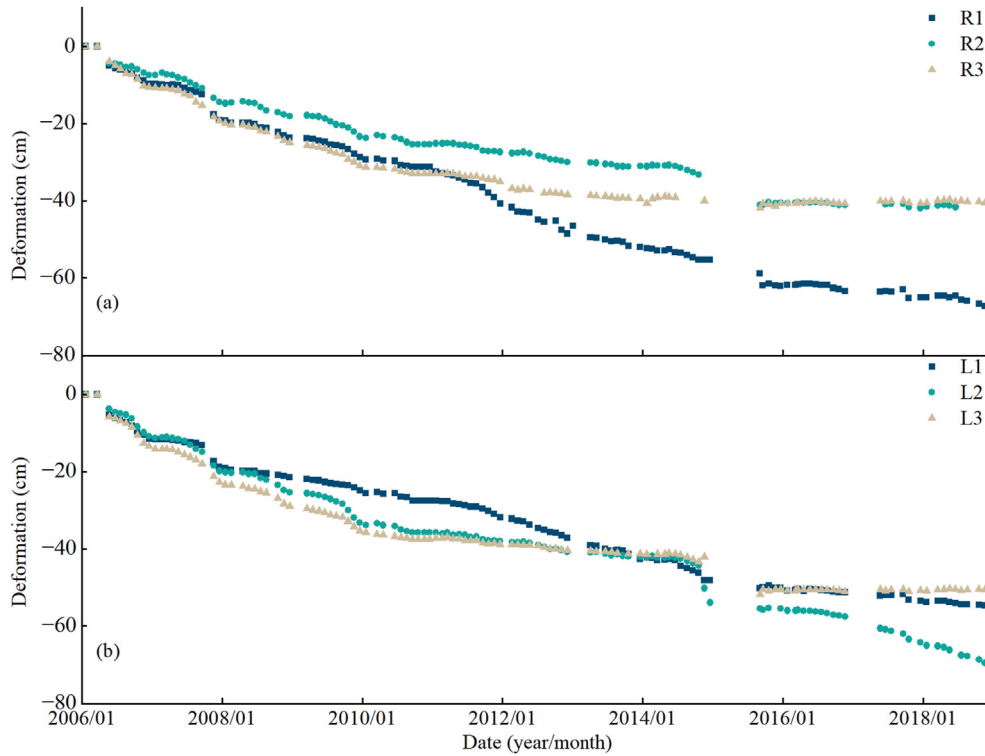


Fig. 9. Settlement processes of the (a) right shoulder and (b) left shoulder of the embankment at K1497 + 150.

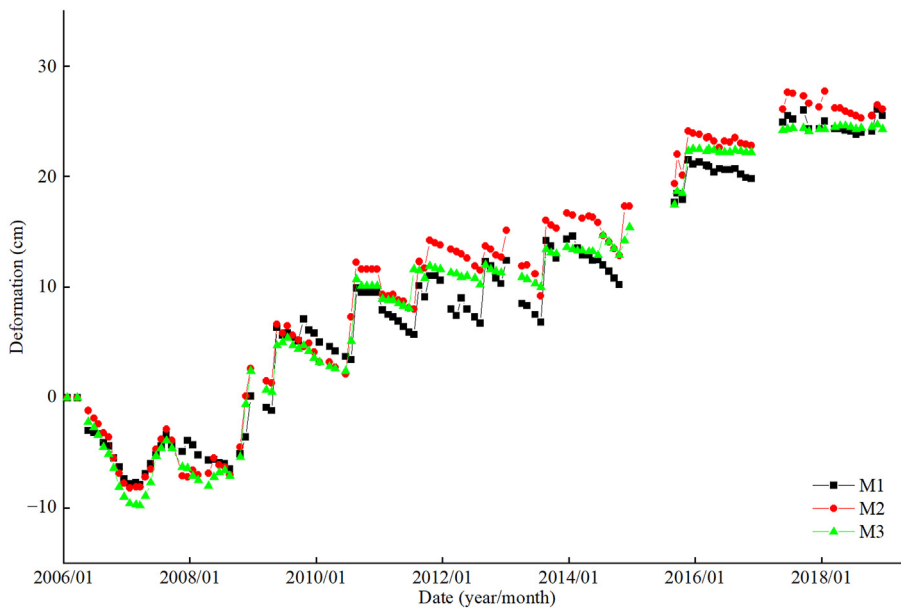


Fig. 10. Settlement processes of the embankment centre at K1497 + 150 in 2006–2018.

effect from the CRR in the warm season and the cooling function from the thermosyphons in the cold season strengthened the cooling effect on the embankment in warm permafrost regions.

At experimental section K1497 + 150, there was a 1.1 m thick layer of warm ice-saturated permafrost under the embankment, which caused the embankment to settle and deform as the ground temperature rose. The embankment

deformation has been monitored since three years after its construction. The embankment settlement during this period mainly originated from compaction after thawing and creep of the underlying warm and ice-rich permafrost layers, excluding the compaction of the roadbed filler and the active layer (Ma et al., 2012). Under the left shoulder of the embankment, for example, the permafrost table fell 0.46 m between 2006 and 2010, and the ground temperatures showed that thawing

mainly occurred in the ice-saturated permafrost layer. After the strengthening measures were installed in 2010 and 2012, the deformation rate of the embankment decreased significantly along with the decrease of permafrost temperature. The deformation rate is currently very close to zero. Again, it has been shown that the coupled strengthening measures of the CRR and thermosyphons could have a significant cooling effect on the embankment and effectively reduce the deformation rate of the embankment.

Under the left shoulder, the ground temperature at the bottom of the permafrost layer rose rapidly, and the permafrost base raised by 1.89 m from 2016 to 2018 (Fig. 5). The lack of up-to-date geological information at this section makes it impossible to analyse the cause of the anomaly. A reasonable explanation for this rapid degradation of permafrost is global warming. The ground temperature at the natural site gradually increased to higher than that under the embankment at the same depth after installation of the engineering measures, resulting in heat flowing into the embankment from the side. Meanwhile, the cooling effect of the thermosyphons on the upper permafrost is noticeable, which increased the warming rate of permafrost at the lower part faster than that of the upper layer. In 2017–2018, the warming rate at a depth of 15 m was 0.059 °C per year, which was higher than 0.013 °C per year at a depth of 12 m. At present, significant degradation of permafrost is occurring in the area of the ice-poor permafrost layer with less than 10% volumetric ice content; therefore, degradation of the permafrost in this area has not been causing a serious deformation of the embankment (Fig. 9). However, although the temperature has increased gradually in the lower layer of the permafrost, the thermal disturbance will inevitably affect the ice-saturated permafrost, which will cause a significant deformation of the embankment. Therefore, countermeasures should be taken as soon as possible based on the analysis of the warming process and further geological exploration.

5. Conclusions

Based on the analysis of ground temperature and deformation measured at section K1497 + 150, the following conclusions can be drawn:

- (1) The permafrost in this area is degrading as a result of climate warming. Before the strengthening measures of the CRR and thermosyphons were installed, the permafrost under the embankment degraded faster than that under the natural site because of the superposition influence of the roadbed engineering. The permafrost table under the natural site descended at a rate of 0.054 m per year from 2006 to 2009, much lower than that under the left shoulder, which was 0.09 m per year.
- (2) This study shows that the strengthening measures of the CRR and thermosyphons could effectively improve the stability of the embankment in the warm and ice-rich permafrost region under climate warming. The CRR slows the rising rate of the ground temperature by

preventing heat transfer to the embankment in the summer. However, its ability to cool permafrost far from the crushed rock layer is weak, meaning that the CRR commonly used to strengthen the QTR may not be effective in preventing degradation of underlying permafrost in warm and ice-rich regions under climate change. The cooling ability of the thermosyphons in the winter helps increase the cold storage inside of the embankment, which is conducive to permafrost resisting the influences of environmental warming. The coupling of the two measures makes the cooling capacity much stronger than that of a single one. The monitoring results of this study confirmed that, even in a warm permafrost region, the coupled strengthening measures can effectively improve the thermal stability of the permafrost at different depths under the embankment and can reduce the settlement deformation of the embankment.

Declaration of competing interest

The authors declare no conflict of interest.

Acknowledgments

We would like to express our gratitude to two anonymous reviewers for their constructive comments and suggestions. This study was supported by the Strategic Priority Research Program of the Chinese Academy of Science (XDA20020102), Science and Technology Project of State Grid Corporation of China (SGQHDKYOSBJS201600077), the Natural Science Foundation of China (41101065), and the State Key Laboratory of Frozen Soils Engineering Foundation (SKLFS-ZT-34).

References

- Cheng, G., 2002. Interaction between Qinghai–Tibet Railway engineering and permafrost and environmental effects. *Bull. Chin. Acad. Sci.* 17 (1), 21–25. <https://doi.org/10.16418/j.issn.1000-3045.2002.01.006> (Chinese).
- Cheng, G., 2005. A roadbed cooling approach for the construction of Qinghai–Tibet Railway. *Cold Reg. Sci. Technol.* 42, 169–176. <https://doi.org/10.1016/j.coldregions.2005.01.002>.
- Cheng, G., He, P., 2001. Linear engineering construction in permafrost regions. *J. Glaciol. Geocryol.* 23 (3), 213–217. <https://doi.org/10.3969/j.issn.1000-0240.2001.03.001> (Chinese).
- Cheng, G., Wu, T., 2007. Responses of permafrost to climate change and their environmental significance, Qinghai–Tibet Plateau. *J. Geophys. Res. Earth Surf.* 112, 1–10. <https://doi.org/10.1029/2006JF000631>.
- Hou, Y., Wu, Q., Niu, F., et al., 2015a. Thermal stabilization of duct-ventilated railway embankments in permafrost regions using ripped-rock revetment. *Cold Reg. Sci. Technol.* 120, 145–152. <https://doi.org/10.1016/j.coldregions.2015.10.002>.
- Hou, Y., Wu, Q., Liu, Y., et al., 2015b. The thermal effect of strengthening measures in an insulated embankment in a permafrost region. *Cold Reg. Sci. Technol.* 116, 49–55. <https://doi.org/10.1016/j.coldregions.2015.04.003>.
- Hou, Y., Wu, Q., Dong, J., et al., 2018. Numerical simulation of efficient cooling by coupled RR and TCPT on railway embankments in permafrost

- regions. *Appl. Therm. Eng.* 133, 351–360. <https://doi.org/10.1016/j.applthermaleng.2018.01.070>.
- Li, S., Wang, Z., Zhang, Y., et al., 2016. Comparison of socioeconomic factors between surrounding and non-surrounding areas of the Qinghai—Tibet Railway before and after its construction. *Sustainability* 8, 776. <https://doi.org/10.3390/su8080776>.
- Li, S., Gong, J., Deng, Q., et al., 2018. Impacts of the Qinghai—Tibet Railway on accessibility and economic linkage of the third pole. *Sustainability* 10, 1–17. <https://doi.org/10.3390/su10113982>.
- Ma, W., Cheng, G., Wu, Q., 2009. Construction on permafrost foundations: lessons learned from the Qinghai—Tibet railroad. *Cold Reg. Sci. Technol.* 59, 3–11. <https://doi.org/10.1016/j.coldregions.2009.07.007>.
- Ma, W., Feng, G., Wu, Q., et al., 2008. Analyses of temperature fields under the embankment with crushed-rock structures along the Qinghai—Tibet Railway. *Cold Reg. Sci. Technol.* 53, 259–270. <https://doi.org/10.1016/j.coldregions.2007.08.001>.
- Ma, W., Wen, Z., Sheng, Y., et al., 2012. Remedying embankment thaw settlement in a warm permafrost region with thermosyphons and crushed rock revetment. *Can. Geotech. J.* 49, 1005–1014. <https://doi.org/10.1139/T2012-058>.
- Mu, Y., Ma, W., Wu, Q., et al., 2012. Thermal regime of conventional embankments along the Qinghai—Tibet Railway in permafrost regions. *Cold Reg. Sci. Technol.* 70, 123–131. <https://doi.org/10.1016/j.coldregions.2011.08.005>.
- Mu, Y., Ma, W., Niu, F., et al., 2018. Long-term thermal effects of air convection embankments in permafrost zones: case study of the Qinghai—Tibet Railway, China. *J. Cold Reg. Eng.* 32, 1–10. [https://doi.org/10.1061/\(ASCE\)CR.1943-5495.0000166](https://doi.org/10.1061/(ASCE)CR.1943-5495.0000166).
- Peng, H., Ma, W., Mu, Y., et al., 2015. Degradation characteristics of permafrost under the effect of climate warming and engineering disturbance along the Qinghai—Tibet Highway. *Nat. Hazards* 75 (3), 2589–2605.
- Ran, Y., Li, X., Cheng, G., 2018. Climate warming over the past half century has led to thermal degradation of permafrost on the Qinghai—Tibet Plateau. *Cryosphere* 12, 595–608. <https://doi.org/10.5194/tc-12-595-2018>.
- Shi, Y., Mi, W., 2018. Map of Snow, Ice, and Frozen Ground in China. National Cryosphere Desert Data Center. <http://www.ncdc.ac.cn/>.
- Sun, Z., Ma, W., Zhang, S., et al., 2018. Embankment stability of the Qinghai—Tibet Railway in permafrost regions. *J. Cold Reg. Eng.* 32, 1–7. [https://doi.org/10.1061/\(ASCE\)CR.1943-5495.0000153](https://doi.org/10.1061/(ASCE)CR.1943-5495.0000153).
- Wang, H., Sun, Z., Liu, Y., et al., 2018. Thermal state of embankment with thawed interlayer in permafrost regions of the Qinghai—Tibet Railway. *J. Glaciol. Geocryol.* 40 (5), 934–942. <https://doi.org/10.7522/j.issn.1000-0240.2018.0508> (Chinese).
- Wang, S., Jin, H., Li, S., et al., 2000. Permafrost degradation on the Qinghai—Tibet Plateau and its environmental impacts. *Permafr. Periglac. Process.* 11, 43–53. [https://doi.org/10.1002/\(SICI\)1099-1530\(200001/03\)11:1<43::AID-PPP332>3.0.CO;2-H](https://doi.org/10.1002/(SICI)1099-1530(200001/03)11:1<43::AID-PPP332>3.0.CO;2-H).
- Wen, Z., Sheng, Y., Ma, W., et al., 2005. Analysis on effect of permafrost protection by two-phase closed thermosyphon and insulation jointly in permafrost regions. *Cold Reg. Sci. Technol.* 43, 150–163. <https://doi.org/10.1016/j.coldregions.2005.04.001>.
- Wu, Q., Zhang, T., 2008. Recent permafrost warming on the Qinghai—Tibetan Plateau. *J. Geophys. Res. Atmos.* 113, 1–22. <https://doi.org/10.1029/2007JD009539>.
- Wu, Q., Zhang, T., 2010. Changes in active layer thickness over the Qinghai—Tibetan Plateau from 1995 to 2007. *J. Geophys. Res.* 115, 1–12. <https://doi.org/10.1029/2009jd012974>.
- Wu, Q., Niu, F., 2013. Permafrost changes and engineering stability in Qinghai—Xizang Plateau. *Chin. Sci. Bull.* 58, 1079–1094. <https://doi.org/10.1007/s11434-012-5587-z>.
- Wu, Q., Liu, Y., Yu, H., 2007. Analysis of the variations of permafrost under ordinary embankment along the Qinghai—Tibet Railway. *J. Glaciol. Geocryol.* 29 (6), 960–969. <https://doi.org/10.1007/s11442-007-0020-2> (in Chinese).
- Wu, Q., Li, M., Liu, Y., 2011. Thermal interaction between permafrost and the Qinghai—Tibet railway. *J. Cold Reg. Eng.* 24, 112–125.
- Wu, Q., Liu, Y., Zhang, J., et al., 2002. A review of recent frozen soil engineering in permafrost regions along Qinghai—Tibet Highway, China. *Permafr. Periglac. Process.* 13, 199–205. <https://doi.org/10.1002/ppp.420>.
- Yan, Z., Zhang, M., Lai, Y., et al., 2019. Countermeasures combined with thermosyphons against the thermal instability of high-grade highways in permafrost regions. *Int. J. Heat Mass Transf.* 119047. <https://doi.org/10.1016/j.ijheatmasstransfer.2019.119047>.
- Yu, W., Liu, W., Chen, L., et al., 2016. Evaluation of cooling effects of crushed rock under sand-filling and climate warming scenarios on the Tibet Plateau. *Appl. Therm. Eng.* 92, 130–136. <https://doi.org/10.1016/j.applthermaleng.2015.09.030>.
- Zhang, Z., Wu, Q., Jiang, G., et al., 2020. Changes in the permafrost temperatures from 2003 to 2015 in the Qinghai—Tibet Plateau. *Cold Reg. Sci. Technol.* 169, 102904. <https://doi.org/10.1016/j.coldregions.2019.102904>.
- Zhao, H., Wu, Q., Zhang, Z., 2019. Long-term cooling effect of the crushed rock structure embankments of the Qinghai—Tibet Railway. *Cold Reg. Sci. Technol.* 160, 21–30. <https://doi.org/10.1016/j.coldregions.2019.01.006>.